LOW EARTH ORBIT SATELLITE RAIN ATTENUATION ANALYSIS: CASE STUDY OF IRIDIUM 914 SATELLITE

Ogungbemi Emmanuel Oluropo[1]
Dept. of Electrical/Electronic & Computer Engineering, University of Uyo, Nigeria

Israel Sylvester Umana[2]
Dept. of Electrical/Electronic & Computer Engineering, University of Uyo, Nigeria

Akpasam Joseph Ekanem[3]
Department of Electrical and Electronic Engineering, Akwa Ibom State University Mkpat Enin, Akwa Ibom State, Nigeria

Abstract— In this paper, low earth orbit satellite rain attenuation analysis is presented. The case study is Iridium 914 satellite and the earth station is at University of Uyo at latitude of 5.028933° , longitude of 7.978991° and magnetic declination of 0° 52' W. The orbital track data with respect to the earth station gave elevation angles in the range of 10°to 74°. The International Telecommunication Union (ITU) power-law model which expresses rain attenuation in terms of specific rain attenuation and some frequency and polarization dependents parameters was used. The results show that the specific rain attenuation is not affected by the elevation angle but it is affected by the signal polarization. Accordingly, the specific rain attenuation for the horizontal polarized signal is higher for all the elevation angles than that of the vertical polarized signal. Also, the results show that the rain attenuation is inversely proportional to elevation angle. Hence, the rain attenuation is high for low elevation angle but low for high elevation angle. Furthermore, the rain attenuation for the horizontal polarized signal is higher for all the elevation angles than that of the vertical polarized signal. In addition, the rain attenuation is inversely proportional to rain fall exceeded percentages, P. Hence, the rain attenuation is high for low P but low for high P. In all, in this paper, the ideas presented is very relevant to satellite link designers in the selection of equipment and parameter values for different rain zones and desired network availability.

Keywords— Low Earth Orbit Satellite, Rain Attenuation, Network Availability, Specific Rain Attenuation, Iridium 914 Satellite, Magnetic Declination, Power-Law Model, Polarized Signal

1. Introduction

Today, satellite technologies have become widely adopted in diverse applications that include remote sensing, weather forecasting, reconnaissance, navigation, and various forms of communications [1,2,3,4,5,6,7,8,9,10]. The specific application determines the type of satellite to be deployed. In this paper, the Iridium satellite is considered. Basically, the Iridium satellite is a constellation of about 66 satellites that are used to provide global coverage for voice and data communication among handheld mobile devices [11,12,13,14,15,16,171,18,19,20]. Such communication system utilizes wireless signal in the high frequency microwave bands which are significantly affected by rain attenuation [21,22,23,24,25,26,27,28]. As such, the quality of service of such satellite link can be effected by rainfall in the regions where the earth stations are located.

Again, Iridium satellite is a Low Earth Orbit (LEO) satellite which means that its position relative to a given earth station changes with time [29,30,31,32,33,34]. The changing position entails changes in the elevation angle which also affect other parameters of the rain attenuation that can be suffered by the wireless signal used in the satellite link. Accordingly, in this paper, the analysis of the rain attenuation of the Iridium satellite-earth station link is conducted. The analysis used satellite tracking dataset to determine the position and the corresponding elevation angles of the Iridium satellite over its repeat cycle. The analysis considered the variation of the specific rain attenuation , the effective rain path length and the rain attenuation with elevation angles of the Iridium satellite link relative to a given earth station location. Matlab software was used to carry out the computations.

2. Methodology

The model used is the International Telecommunication Union (ITU) ***power-law*** rain attenuation computation model which expresses rain attenuation in terms of specific rain attenuation and some frequency and polarization dependents parameters, along with effective rain path length. However, the effective rain path length is determined from the rain slant path length, L_s and L_g which is the horizontal projection distance covered by L_s , as shown in Figure 1.

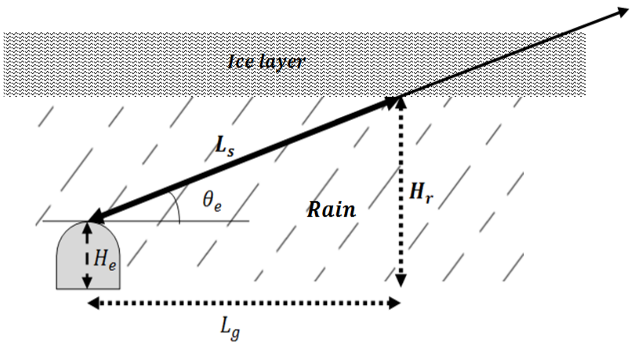

Figure 1 The diagram for modelling the rain slant path length, L_s

The rain attenuation for horizontally or vertically polarized signal is considered. Let the specific rain attenuation for vertically polarized signal be denoted as γ_v, then ;

$$\gamma_v = k_v \ (R_p)^{\alpha_v} \quad (1)$$

Let the specific rain attenuation for horizontal polarized signal be denoted as γ_h, then ;

$$\gamma_h = k_h \ (R_p)^{\alpha_h} \quad (2)$$

Where the values of the parameters, k_v, α_v ' k_h and α_h depend on the frequency and the the signal polarization category. The rain slant path length, L_s is given in terms of rain height (H_r), the earth station altitude or height (H_e) and the satellite link elevation angle (θ_e) as follows;

$$L_s = \frac{H_r - H_e}{\sin(\theta_e)} \quad (3)$$

The horizontal projection distance covered by L_s on the ground is denoted as L_g where;

$$L_g = (L_s)\cos(\theta_e) \quad (4)$$

The rain path length reduction factor, (r_p) for different rain fall exceeded percentages, P is computed as follows;

$$r_p = \begin{cases} \frac{10}{10+L_g} & for\ p = 0.001\% \\ \frac{90}{90+4(L_g)} & for\ p = 0.01\% \\ \frac{180}{180+L_g} & for\ p = 0.1\% \\ 1 & for\ p = 1\% \end{cases} \quad (5)$$

Let the effective rain path length be denoted as L_e , then ;

$$L_e = L_s(r_p) = \left(\frac{H_r - H_e}{\sin(\theta_e)}\right)(r_p) \quad (6)$$

Let the rain attenuation for horizontally or vertically polarized signal be denoted as A_R, then;

$$A_R = \begin{cases} L_s(r_p)\gamma_v & \text{for vertically polarized signal} \\ L_s(r_p)\gamma_h & \text{for horizontally polarized signal} \end{cases} \quad (7)$$

$$A_R = \begin{cases} L_e(r_p)(k_v\ (R_p)^{\alpha_v}) & \text{for vertically polarized signal} \\ L_e(r_p)(k_h\ (R_p)^{\alpha_h}) & \text{for horizontally polarized signal} \end{cases} \quad (8)$$

Let $A_{R0.01}$ denote rain attenuation computed at p = 0.01 % , where $A_{R0.01}$ is in dB, then rain attenuation at other values of p can be obtained as follows, ;

$$A_{R_P} = \begin{cases} A_{R0.01}\left(0.12p^{-(0.546 + 0.043(Log(p)))}\right) & for\ Lat_{es} \geq 30° \\ A_{R0.01}\left(0.07p^{-(0.855 + 0.139(Log(p)))}\right) & for\ Lat_{es} < 30° \end{cases} \quad (9)$$

Where Lat_{es} is the latitude of the earth station.

The case study LEO satellite is IRIDIUM 914 and the summary of key parameters of the satellite are presented in Table 1. The earth station is at University of Uyo , Aka Ibom Nigeria, with latitude of 5.028933° , longitude of 7.978991° and magnetic declination of 0° 52' W. The IRIDIUM 914 10-day live tracking predictions dataset based on earth station observation location coordinates of 5.028933, 7.978991is presented in Table 2 and Figure 2. Based on the dataset in Table 1, the following elevation angles are used : 10°, 18°, 26°, 41°,49°, 52°,60°,69° and 74°. Also, the rainfall rates exceeding 0.01% of an average year in Uyo is 124 mm/hr [35]. Also, Iridium operates in the L-band frequency of **1 – 2 GHz**

Table 1 The launch detail and orbital elements of IRIDIUM 914

Launch Detail	
Launched	18 June 1997
Status	Non-operational
Category	Iridium
Launch site	Tyuratam Missile and Space Center, Kazakhstan (Also known as Baikonur Cosmodrome)
Owner	United States
NORAD ID	24836
COSPAR ID	1997-030A
Current orbital elements	
Inclination	86.391°
Eccentricity	0.00037
RA ascending node	6.450 hr
Argument perihelion	105.492°
Mean anomaly	254.669°
Orbital period	100.071 min
Epoch of osculation	05 May 2021, 22:31

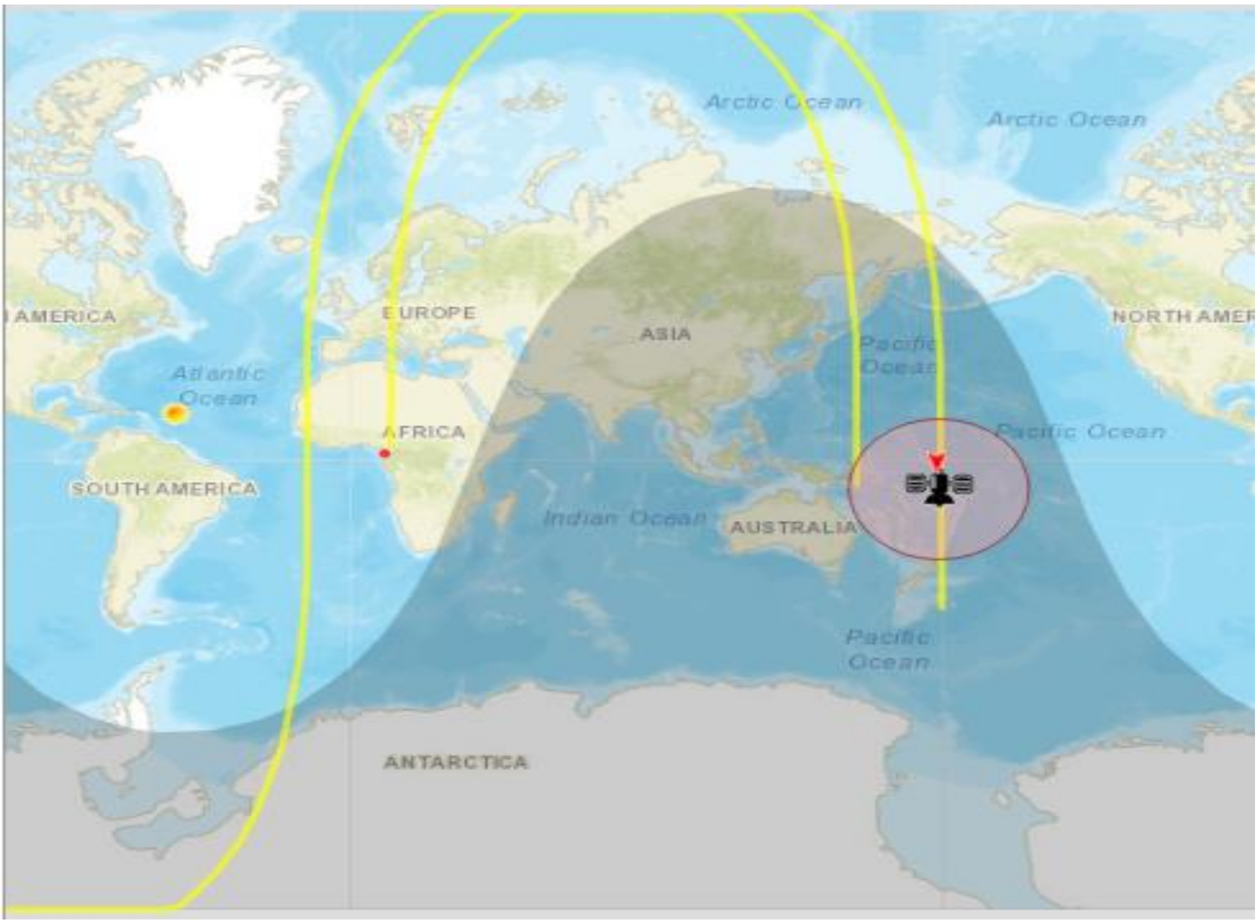

Figure 2 IRIDIUM 914 live tracking predictions map showing the orbit track (yellow line) , the ground foot print of the satellite and the earth station

Table 2 IRIDIUM 914 10-day live tracking predictions dataset based on earth station observation location coordinates of 5.028933, 7.978991

Start		Max altitude			End		All passes
Date, Local time	Az	Local time	Az	El	Local time	Az	Mag
8-May 03:57	N 351°	**04:04**	**W 274°**	**52°**	04:11	S 190°	+9.5
8-May 14:51	SSE 154°	**14:58**	**E 90°**	**23°**	15:04	NNE 24°	+8.5
8-May 16:31	SSW 209°	**16:38**	**W 271°**	**19°**	16:44	NNW 333°	+8.7
9-May 03:18	N 7°	**03:26**	**E 92°**	**60°**	03:33	S 173°	+9.6
9-May 15:52	S 191°	**16:00**	**W 270°**	**49°**	16:07	N 350°	+7.4
10-May 02:41	NNE 23°	**02:48**	**E 89°**	**23°**	02:54	SSE 154°	+9.9
10-May 04:21	NNW 333°	**04:28**	**W 273°**	**19°**	04:34	SW 211°	+9.9
10-May 15:14	S	**15:21**	**E**	**63°**	15:29	N	+7.1

Start		Max altitude			End		All passes
Date, Local time	Az	Local time	Az	El	Local time	Az	Mag
	173°		94°			6°	
11-May 03:42	N 350°	**03:50**	**W 271°**	**48°**	03:57	S 192°	+9.8
11-May 14:37	SSE 156°	**14:43**	**E 88°**	**24°**	14:50	NNE 23°	+8.4
11-May 16:17	SW 210°	**16:23**	**W 270°**	**18°**	16:30	NNW 331°	+8.8
12-May 03:04	N 5°	**03:11**	**E 85°**	**65°**	03:19	S 174°	+9.9
12-May 15:38	S 192°	**15:45**	**W 272°**	**45°**	15:52	N 349°	+7.5
13-May 02:27	NNE 22°	**02:33**	**E 91°**	**25°**	02:40	SSE 156°	-
13-May 04:07	NNW 331°	**04:13**	**W 272°**	**17°**	04:20	SW 213°	-
13-May 15:00	S 175°	**15:07**	**E 89°**	**69°**	15:14	N 5°	+7.1
14-May 03:28	N 348°	**03:35**	**W 269°**	**44°**	03:42	S 193°	-
14-May 14:22	SSE 157°	**14:29**	**E 90°**	**26°**	14:36	NNE 22°	+8.3
14-May 16:03	SW 213°	**16:09**	**W 271°**	**17°**	16:15	NW 329°	+8.9
15-May 02:50	N 4°	**02:57**	**E 90°**	**71°**	03:04	S 176°	-
15-May 15:24	S 193°	**15:31**	**W 269°**	**42°**	15:38	N 347°	+7.7
16-May 02:12	NNE 20°	**02:19**	**E 89°**	**27°**	02:26	SSE 157°	-
16-May 03:53	NW 329°	**03:59**	**W 271°**	**16°**	04:05	SW 214°	-
16-May 14:46	S 176°	**14:53**	**E 80°**	**74°**	15:00	N 3°	+7.0
17-May 01:36	NE 41°	**01:41**	**E 88°**	**10°**	01:46	SE 136°	-
17-May 03:14	N 347°	**03:21**	**W 272°**	**41°**	03:28	S 195°	-
17-May 14:08	SSE 158°	**14:15**	**E 89°**	**28°**	14:22	NNE 20°	+8.2

Legend:	Not visible	Marginal	Good	Excellent

(Source: https://www.n2yo.com/passes/?s=24836)

3. Result and Discussion

The cases study IRIDIUM 914 satellite link elevation angles ranging from 10° to 74° were extracted from a 10-day live tracking predictions dataset based on earth station observation location coordinates of 5.028933, 7.978991. The elevation angles were then used in the analytical expressions presented in this paper to determine the rain slant path length and hence the effective rain path length, as shown in Table 3. The graph plot of the effective rain path length versus elevation angle is given in Figure 3. The results in Table 3 and Figure 3 show that the effective rain path length is inversely proportional to elevation angle. Hence, the effective rain path length is high for low elevation angle but low for high elevation angle.

The results of the computation for the specific rain attenuation as a function of elevation angle are presented in Table 4 and Figure 4. The results in Table 4 and Figure 4 show that the specific rain attenuation is not affected by the elevation angle but it is affected by the signal polarization. Accordingly, the specific rain attenuation for the horizontal polarized signal is higher for all the elevation angles than that of the vertical polarized signal.

The results of the computation for the rain attenuation as a function of elevation angle are presented in Table 5 and Figure 5. The results in Table 5 and Figure 5 show that the rain attenuation is affected by the elevation angle and the signal polarization. Accordingly, the rain attenuation for the horizontal polarized signal is higher for all the elevation angles than that of the vertical polarized signal. The results in Table 5 and Figure 5 show that the rain attenuation is inversely proportional to elevation angle. Hence, the rain attenuation is high for low elevation angle but low for high elevation angle.

The results of the computation for the rain attenuation as a function of elevation angle for different rain fall exceeded percentages, P are presented in Table 6 and Figure 6. The results in Table 6 and Figure 6 show that the rain attenuation is inversely proportional to P. Hence, the rain attenuation is high for low P but low for high P.

Table 3 The results of the computation for the rain slant path length and the effective rain path length

Elevation Angle (θ°)	Rain slant path length , Ls in km	(Lg) Horizontal projection distance of L_S on the ground in km	Rain path length reduction factor, rp	Effective rain path length , Le in km
10	27.3	26.9	0.5	12.4
18	15.4	14.6	0.6	9.3
26	10.8	9.7	0.7	7.6
41	7.2	5.5	0.8	5.8
52	6.0	3.7	0.9	5.2
60	5.5	2.7	0.9	4.9
69	5.1	1.8	0.9	4.7
74	4.9	1.4	0.9	4.7

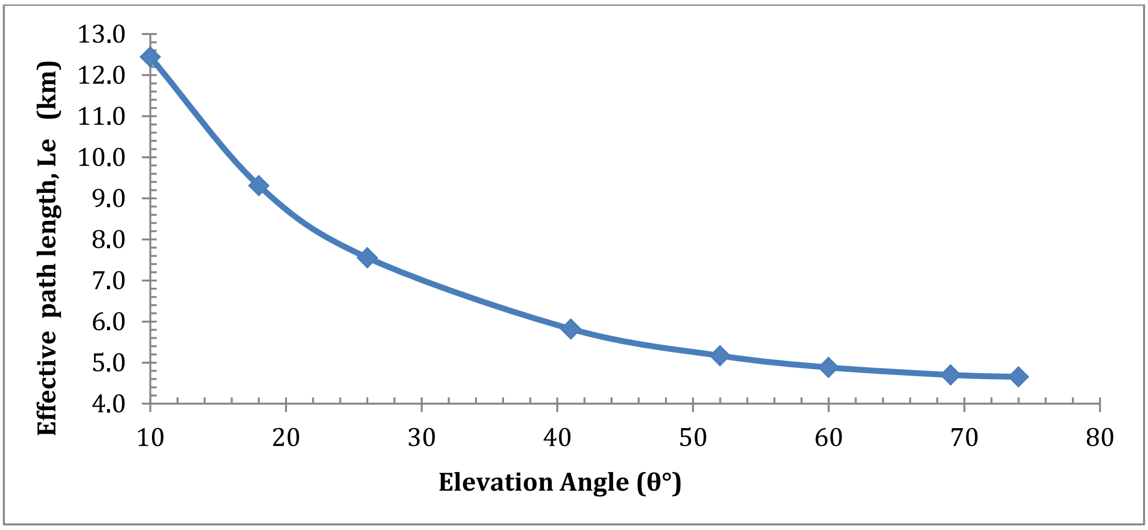

Figure 3 The effective rain path length versus elevation angle

Table 4 The results of the computation for the specific rain attenuation as a function of elevation angle

Elevation Angle (θ°)	Specific Rain Attenuation in dB for horizontal polarization	Specific Rain Attenuation in dB for vertical polarization
10	0.00981	0.00670
18	0.00981	0.00670
26	0.00981	0.00670
41	0.00981	0.00670
52	0.00981	0.00670
60	0.00981	0.00670
69	0.00981	0.00670
74	0.00981	0.00670

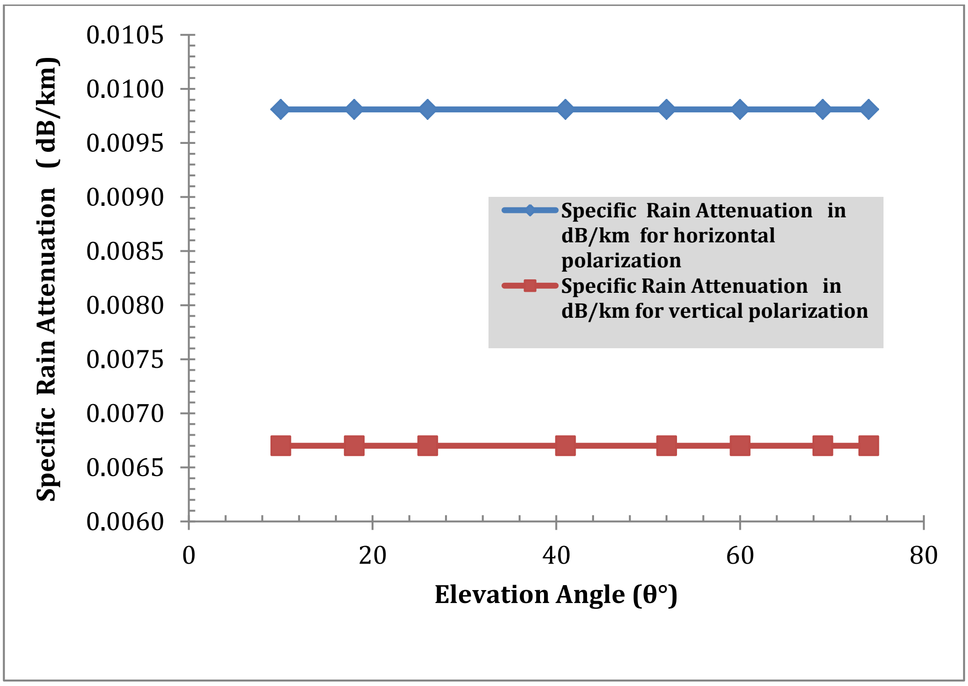

Figure 4 The graph plot for the specific rain attenuation versus elevation angle

Table 5 The results of the computation for the rain attenuation as a function of elevation angle

Elevation Angle (θ°)	Rain Attenuation in dB for horizontal polarization	Rain Attenuation in dB for vertical polarization
10	0.122106	0.083403
18	0.091372	0.06241
26	0.074151	0.050648
41	0.057113	0.03901
52	0.050726	0.034648
60	0.047926	0.032735
69	0.046136	0.031513
74	0.045673	0.031196

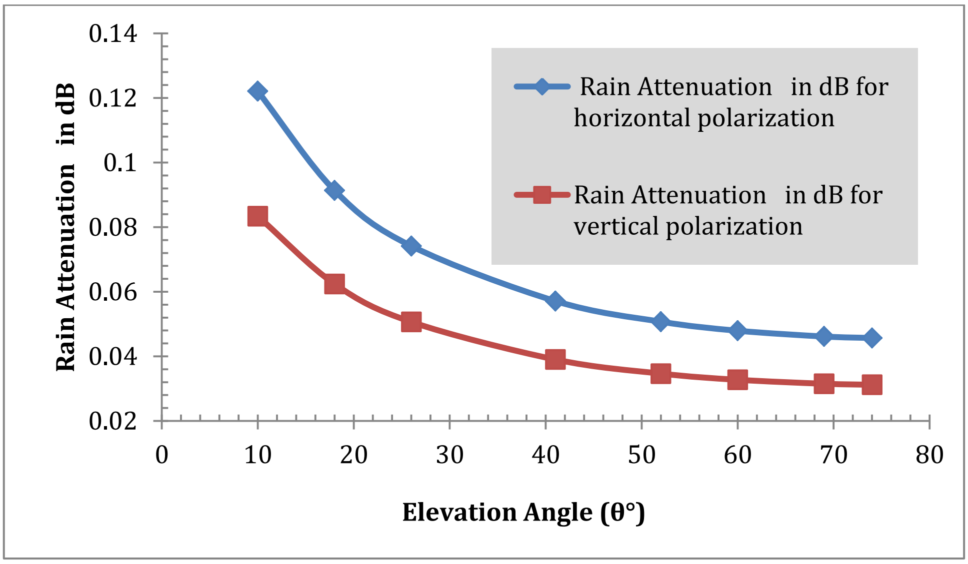

Figure 5 The graph plot for the rain attenuation versus elevation angle

Table 6 The results of the computation for the rain attenuation as a function of elevation angle for different rain fall exceeded percentages, P

Elevation Angle (θ°)	Rain Attenuation (horizontal) in dB for p = 0.001%	Rain Attenuation (vertical) in dB for p = 0.001%	Rain Attenuation (horizontal) in dB for p = 0.01%	Rain Attenuation (vertical) in dB for p = 0.01%	Rain Attenuation (horizontal) in dB for p = 0.1%	Rain Attenuation (vertical) in dB for p = 0.1%	Rain Attenuation (horizontal) in dB for p = 1%	Rain Attenuation (vertical) in dB for p = 1%
10	0.1761	0.1203	0.1221	0.0834	0.0444	0.0304	0.0085	0.0058
18	0.1318	0.0900	0.0914	0.0624	0.0333	0.0227	0.0064	0.0044
26	0.1070	0.0731	0.0742	0.0506	0.0270	0.0184	0.0052	0.0035
41	0.0824	0.0563	0.0571	0.0390	0.0208	0.0142	0.0040	0.0027
52	0.0732	0.0500	0.0507	0.0346	0.0185	0.0126	0.0036	0.0024
60	0.0691	0.0472	0.0479	0.0327	0.0174	0.0119	0.0034	0.0023
69	0.0665	0.0455	0.0461	0.0315	0.0168	0.0115	0.0032	0.0022
74	0.0659	0.0450	0.0457	0.0312	0.0166	0.0114	0.0032	0.0022

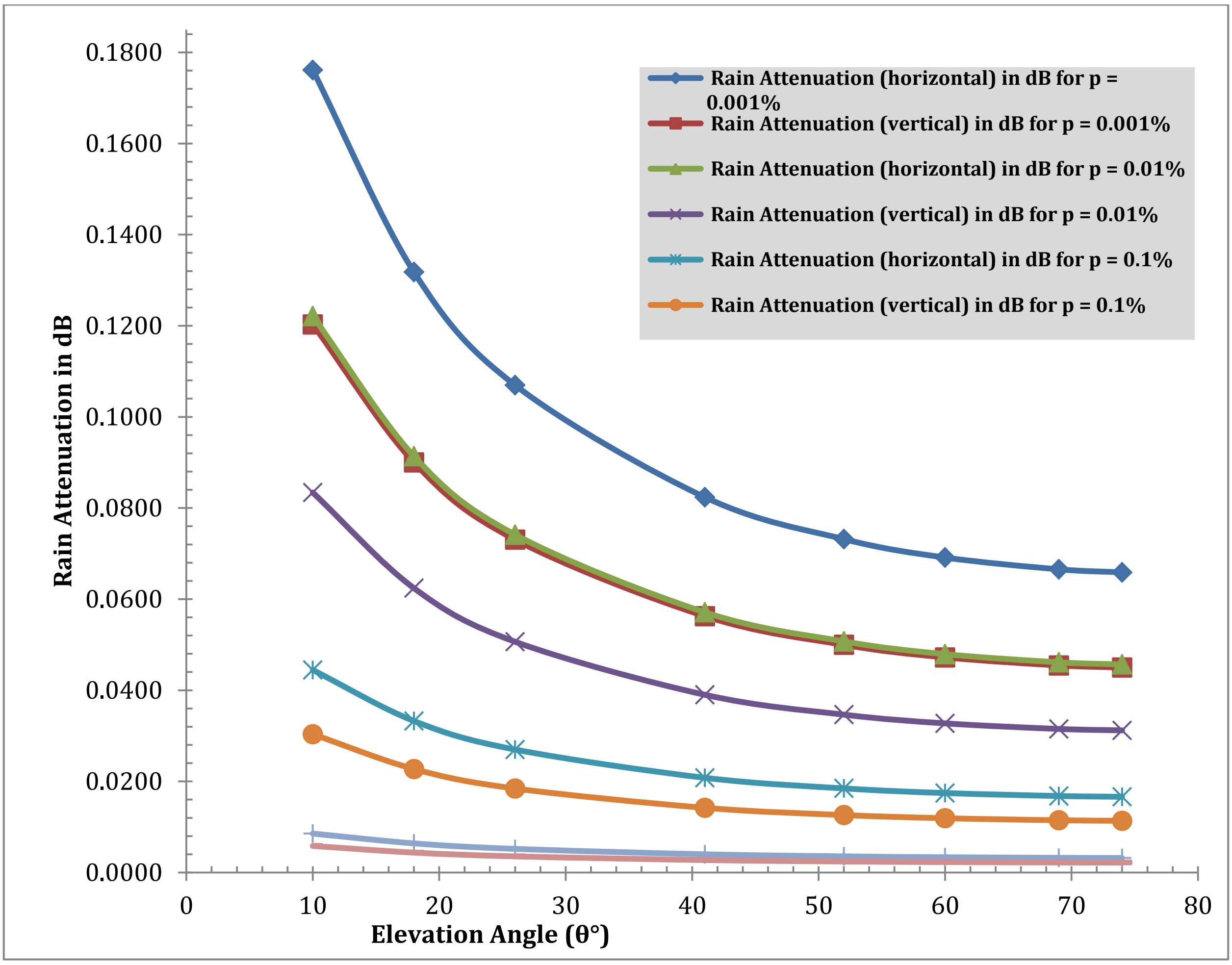

Figure 6 The results of the computation for the rain attenuation as a function of elevation angle for different rain fall exceeded percentages, P

4. Conclusion

Rain attenuation for a LEO satellite for different elevation angles and for different rain fall exceeded percentages, P is studied. The model used is the International Telecommunication Union (ITU) ***power-law*** rain attenuation computation model which expresses rain attenuation in terms of specific rain attenuation and some frequency and polarization dependents parameters, along with effective rain path length. The study also considered the effect of the elevation angle on the effective rain path length, the specific rain attenuation and the rain attenuation. In all, the results showed that the horizontally polarized signal had higher rain attenuation in all the elevation angles than the vertically polarized signal.

References

1. Eshwari, A. P., & Shrivastava, A. K. (2017). Application of Satellite Communication & Remote Sensing for Development. *Journal of Pure Applied and Industrial Physics*, *7*(6), 224-238.
2. Zhu, L., Suomalainen, J., Liu, J., Hyyppä, J., Kaartinen, H., & Haggren, H. (2018). A review: Remote sensing sensors. *Multi-purposeful application of geospatial data*, 19-42.
3. Klemas, V. V. (2015). Coastal and environmental remote sensing from unmanned aerial vehicles: An overview. *Journal of coastal research*, *31*(5), 1260-1267.
4. Toth, C., & Jóźków, G. (2016). Remote sensing platforms and sensors: A survey. *ISPRS Journal of Photogrammetry and Remote Sensing*, *115*, 22-36.
5. Alvarez, J., & Walls, B. (2016, March). Constellations, clusters, and communication technology: Expanding small satellite access to space. In *2016 IEEE Aerospace Conference* (pp. 1-11). IEEE.
6. Homainejad, N., & Rizos, C. (2015). APPLICATION OF MULTIPLE CATEGORIES OF UNMANNED AIRCRAFT SYSTEMS (UAS) IN DIFFERENT AIRSPACES FOR BUSHFIRE MONITORING AND RESPONSE. *International Archives of the Photogrammetry, Remote Sensing & Spatial Information Sciences*, *40*.
7. Sweeting, M. (2018). Modern small satellites-changing the economics of

space. *Proceedings of the IEEE*, *106*(3), 343-361.
8. Razani, M. (2018). *Commercial Space Technologies and Applications: Communication, Remote Sensing, GPS, and Meteorological Satellites*. CRC Press.
9. Guo, F., Fan, Y., Zhou, Y., Xhou, C., & Li, Q. (2014). *Space electronic reconnaissance: localization theories and methods*. John Wiley & Sons.
10. Klimkowska, A., Lee, I., & Choi, K. (2016). Possibilities of UAS for maritime monitoring. *The International Archives of Photogrammetry, Remote Sensing and Spatial Information Sciences*, *41*, 885.
11. Sekiguchi, K. (2016, October). Iridium contributes to "maritime safety". In *2016 Techno-Ocean (Techno-Ocean)* (pp. 90-92). IEEE.
12. Gaur, D., & Prasad, M. S. (2020, June). Satellite Constellation Stationing Effects on Communication Networks. In *2020 8th International Conference on Reliability, Infocom Technologies and Optimization (Trends and Future Directions)(ICRITO)* (pp. 1189-1194). IEEE.
13. Yang, X. (2020). *Low earth orbit (LEO) mega constellations-satellite and terrestrial integrated communication networks* (Doctoral dissertation, University of Surrey).
14. Abo-Zeed, M., Din, J. B., Shayea, I., & Ergen, M. (2019). Survey on land mobile satellite system: Challenges and future research trends. *IEEE Access*, *7*, 137291-137304.
15. Maine, K., Devieux, C., & Swan, P. (1995, November). Overview of IRIDIUM satellite network. In *Proceedings of WESCON'95* (p. 483). IEEE.
16. O'Regan, G. (2016). A Short History of Telecommunications. In *Introduction to the History of Computing* (pp. 151-161). Springer, Cham.
17. Hatlelid, J. E., & Casey, L. (1993). The Iridium (tm) system: Personal communications anytime, anyplace.
18. Reid, T. G., Neish, A. M., Walter, T., & Enge, P. K. (2018). Broadband LEO constellations for navigation. *NAVIGATION, Journal of the Institute of Navigation*, *65*(2), 205-220.
19. Sushko, M. S. (1999). Commercial voice and data mobile satellite systems: support functions for military voice/data communications. In *MILCOM 1999. IEEE Military Communications. Conference Proceedings (Cat. No. 99CH36341)* (Vol. 1, pp. 367-371). IEEE.
20. Guerra, A. G., Ferreira, A. S., Costa, M., Nodar-López, D., & Agelet, F. A. (2018). Integrating small satellite communication in an autonomous vehicle network: A case for oceanography. *Acta Astronautica*, *145*, 229-237.
21. Banday, Y., Rather, G. M., & Begh, G. R. (2019). Effect of atmospheric absorption on millimetre wave frequencies for 5G cellular networks. *IET Communications*, *13*(3), 265-270.
22. Christofilakis, V., Tatsis, G., Chronopoulos, S. K., Sakkas, A., Skrivanos, A. G., Peppas, K. P., ... & Kostarakis, P. (2020). Earth-to-earth microwave rain attenuation measurements: A survey on the recent literature. *Symmetry*, *12*(9), 1440.
23. Shayea, I., Abd. Rahman, T., Hadri Azmi, M., & Arsad, A. (2018). Rain attenuation of millimetre wave above 10 GHz for terrestrial links in tropical regions. *Transactions on Emerging Telecommunications Technologies*, *29*(8), e3450.
24. Kestwal, M. C., Joshi, S., & Garia, L. S. (2014). Prediction of rain attenuation and impact of rain in wave propagation at microwave frequency for tropical region (Uttarakhand, India). *International Journal of Microwave Science and Technology*, *2014*.
25. Shrestha, S., & Choi, D. Y. (2017). Rain attenuation statistics over millimeter wave bands in South Korea. *Journal of Atmospheric and Solar-Terrestrial Physics*, *152*, 1-10.
26. Ugwu, E. B. I., Umeh, M. C., & Ugonabo, O. J. (2015). Microwave propagation attenuation due to earth's atmosphere at very high frequency (VHF) and ultra-high frequency (UHF) bands in Nsukka under a clear–air condition.
27. Hossain, M. S., & Islam, M. A. (2017, February). Estimation of rain attenuation at EHF bands for earth-to-satellite links in Bangladesh. In *2017 International Conference on Electrical, Computer and Communication Engineering (ECCE)* (pp. 589-593). IEEE.
28. Ishii, S., Kinugawa, M., Wakiyama, S., Sayama, S., & Kamei, T. (2016). Rain attenuation in the microwave-to-terahertz waveband. *Wireless Engineering and Technology*, *7*(02), 59.
29. Del Portillo, I., Cameron, B. G., & Crawley, E. F. (2019). A technical comparison of three low earth orbit satellite constellation systems to provide global broadband. *Acta Astronautica*, *159*, 123-135.
30. Yang, Z., Liu, H., Qian, C., Shu, B., Zhang, L., Xu, X., ... & Lou, Y. (2020). Real-Time Estimation of Low Earth Orbit (LEO) Satellite Clock Based on Ground Tracking Stations. *Remote Sensing*, *12*(12), 2050.
31. Shtark, T., & Gurfil, P. (2018). Regional positioning using a low Earth orbit satellite constellation. *Celestial Mechanics and Dynamical Astronomy*, *130*(2), 1-28.
32. Vishwakarma, S., Chauhan, A. S., & Aasma, S. (2014). A Comparative Study of Satellite Orbits as Low Earth Orbit (LEO) and Geostationary Earth Orbit

(GEO). *SAMRIDDHI: A Journal of Physical Sciences, Engineering and Technology*, *6*(02), 99-106.

33. Llop, J. V., Roberts, P. C., Hao, Z., Tomas, L. R., & Beauplet, V. (2014, November). Very low earth orbit mission concepts for earth observation: Benefits and challenges. In *Reinventing Space Conference* (pp. 18-21).
34. Cakaj, S., Kamo, B., Lala, A., & Rakipi, A. (2014). The coverage analysis for low earth orbiting satellites at low elevation. *International Journal of Advanced Computer Science and Applications*, *5*(6).
35. Omotosho, T. V., & Oluwafemi, C. O. (2009). One-minute rain rate distribution in Nigeria derived from TRMM satellite data. *Journal of Atmospheric and Solar-Terrestrial Physics*, *71*(5), 625-633.